Complex networks from space-filling bearings

J. J. Kranz,[1,2,*] N. A. M. Araújo,[3,4,†] J. S. Andrade, Jr.,[1,5,‡] and H. J. Herrmann[1,5,§]

[1]*Computational Physics for Engineering Materials, IfB, ETH Zurich, Wolfgang-Pauli-Strasse 27, CH-8093 Zurich, Switzerland*

[2]*Theoretical Chemical Biology, Institute of Physical Chemistry, Karlsruhe Institute of Technology, Kaiserstrasse 12, D-76131 Karlsruhe, Germany*

[3]*Departamento de Física, Faculdade de Ciências, Universidade de Lisboa, P-1749-016 Lisboa, Portugal*

[4]*Centro de Física Teórica e Computacional, Universidade de Lisboa, P-1749-016 Lisboa, Portugal*

[5]*Departamento de Física, Universidade Federal do Ceará, 60451-970 Fortaleza, Ceará, Brazil*

(Received 19 March 2015; published 6 July 2015)

Two-dimensional space-filling bearings are dense packings of disks that can rotate without slip. We consider the entire first family of bearings for loops of four disks and propose a hierarchical construction of their contact network. We provide analytic expressions for the clustering coefficient and degree distribution, revealing bipartite scale-free behavior with a tunable degree exponent depending on the bearing parameters. We also analyze their average shortest path and percolation properties.

DOI: 10.1103/PhysRevE.92.012802 PACS number(s): 89.75.Hc, 89.75.Da, 45.70.−n

I. INTRODUCTION

Bearings are mechanical dissipative systems of rotors that, when perturbed, relax towards a bearing state, where all touching rotors rotate without slip. When these bearings cover the entire space they are called space-filling bearings [1]. Moreover, if such packings are sheared between moving surfaces, they can be used as a model to explain the existence of regions where tectonic plates can creep on each other for long periods of time without triggering earthquake activity, known as seismic gaps [2]. Space-filling bearings have also been used as a heuristic model for scale-free velocity fields, where the superdiffusion of massive particles can take place [3].

Herrmann *et al.* [1] present a numerical algorithm to construct configurations of two dimensional space-filling bearings of polydisperse disks for loops of four disks on a stripe geometry. They consider an initial configuration of disks of two types (a and b), touching opposite borders of the stripe, such that two disks of the same type never touch. They also define inverse circles centered in the touching point of each disk with the border of the strip. It is then shown that a family of space-filling bearings can be obtained by a sequence of m and n inversions, around the inversion circles of disks a and b, respectively, followed by reflections. Each configuration is then classified by two integer indices m and n. The contact network of a bearing is obtained by mapping it into a graph, where nodes are the disks and links are established between touching disks. In the bearing state, which has no slip, two disks rolling on each other must have an opposite sense of rotation. The contact networks are thus bipartite, with the type of node defined by its sense of rotation.

Andrade *et al.* [4] have shown that the contact network of Apollonian packings is a scale-free, small-world, Euclidean, space-filling, and matching graph. The interesting properties of this network, called an Apollonian network, have motivated a series of follow-ups to study their geometrical [5], magnetic [6–8], spectral [9], and dynamical properties [10,11]. Even an extension to random networks has been proposed [12]. In contrast to bearings where loops are necessarily of an even number of disks, for the Apollonian network loops are of size three.

Here, we consider the first family of space-filling bearings in the stripe geometry and analyze their contact networks. Doye and Massen looked at these networks in the limit $m = n$ and provided heuristic arguments to estimate their degree exponent [5]. We propose a hierarchical construction of such networks for the entire range of indices m and n. Using such a construction we obtain analytic expressions for the degree distribution and clustering coefficient. We also characterize the shortest path and percolation transition. The topological properties of the contact network are intimately related to the force chains [13] and the dynamical response of the bearing to perturbations [14]. Thus, this work is expected to contribute to future studies of these properties. The paper is organized as follows. In Sec. II we start with the special case $m = n = 0$. The general case is discussed in Sec. III. We finally draw some conclusions in Sec. IV.

II. NETWORK FOR $m = n = 0$

A. The network construction

We begin with the specific case of the space-filling bearing of $m = n = 0$ (see Fig. 1). This bearing has translational symmetry with a unit cell composed of two topologically identical loops of four disks, defined by the largest disks, where the top and bottom surfaces are treated as disks of infinite radius. For $m = n$ the bearing has also $C2$ rotation symmetry around the center of the common edge of the two largest loops. Thus, it is sufficient to consider the hierarchical construction rule for the contact network of one loop in the unit cell. By construction, all loops consist of an even number of disks and the network is bipartite, with two types of nodes denoted as a and b nodes. The construction rule is summarized in Fig. 2. One starts with a loop arrangement of four nodes (two a and two

*j.kranz@kit.edu
†nmaraujo@fc.ul.pt
‡soares@fisica.ufc.br
§hans@ifb.baug.ethz.ch

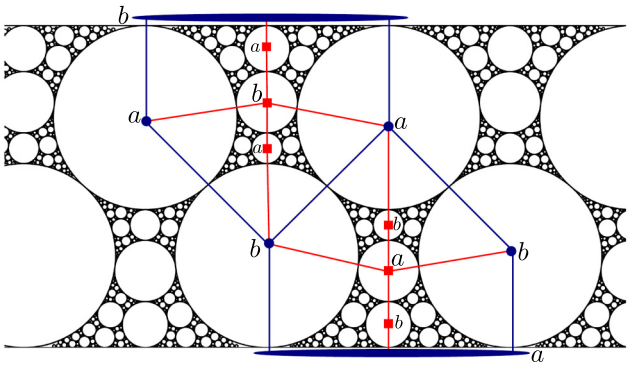

FIG. 1. (Color online) Section of the $m,n = 0$ bearing and the first generation of its contact network. All loops of touching disks consist of an even number of disks and the network is bipartite; i.e., one can label the nodes as a and b such that two touching nodes are always of a different type.

b nodes), corresponding to the four disks of the largest loop. An a node is only connected to b nodes. The first generation $g = 1$ is constructed by adding an a node to the center of the loop and connecting it to the two b nodes, splitting the loop into two loops. This new a node corresponds to the central disk touching the two lateral ones in each loop of the unit cell shown in Fig. 1. Inside each loop one b node is included and connected to the two closest a nodes. These two new nodes correspond to the other two disks vertically aligned with the previous one. At the end, the initial square is divided into four loops. The next generations are obtained hierarchically by repeating the same procedure inside each loop. By construction, the contact network is planar and self-similar.

B. Degree distribution

We now provide an analytic expression for the degree distribution $P(k)$, where k is the node degree (number of touching disks). Let us start with the number of nodes, $N(g)$, at generation g, and neglect the first four nodes. One starts with one loop of two a and two b nodes at generation zero. At each generation, each loop is divided into four. Thus, the final number of loops is 4^g. For each loop in generation $g-1$, one a and two b nodes are added to obtain the generation g, so that the number of a nodes N_a changes from generation $g-1$ to g as

$$\Delta N_a(g) = 4^{g-1} \tag{1}$$

and the number of b nodes N_b as

$$\Delta N_b(g) = 2 \times 4^{g-1} \ . \tag{2}$$

The number of nodes at generation g is then

$$N_a(g) = \sum_{t=1}^{g} 4^{t-1} = \frac{4^g - 1}{3} \tag{3}$$

and

$$N_b(g) = \sum_{t=1}^{g} 2 \times \ 4^{t-1} = \frac{2(4^g - 1)}{3}, \tag{4}$$

respectively. The total number of nodes, N, is

$$N(g) = N_a(g) + N_b(g) = 4^g - 1. \tag{5}$$

At each generation, all a and b nodes receive one new link for each adjacent loop. Since the number of such loops equals the degree, the latter doubles at each generation. The new a nodes have degree 4, while the b nodes have degree 2. Hence, at generation g, the degree $k(t)$ of a node, added at generation g_0 that is part of the network for $t = g - g_0$ generations, is

$$k_a(g - g_0) = 4 \times \ 2^{g-g_0}, \tag{6}$$

$$k_b(g - g_0) = 2 \times \ 2^{g-g_0}. \tag{7}$$

At generation g the degree of a node is related to the generation g_0 at which the node was added. This generation is given by

$$g - g_{0a}(k) = \frac{\ln(k/2)}{\ln 2} - 1, \tag{8}$$

and

$$g - g_{0b}(k) = \frac{\ln(k/2)}{\ln 2}. \tag{9}$$

The number of nodes of degree k at generation g equals the number of nodes added at generation $g_0(k)$, given by Eqs. (1) and (2). Thus, the degree distribution $P_a(k,g)$ is

$$P_a(k,g) = \frac{\Delta N_a(g_{0a}(k))}{N_a(g)} = 3\frac{4^g}{4^g - 1}\left(\frac{k}{2}\right)^{-2}. \tag{10}$$

In the same way, $P_b(k,g)$ is

$$P_b(k,g) = \frac{\Delta N_b(g_{0b}(k))}{N_b(g)} = \frac{3}{4}\frac{4^g}{4^g - 1}\left(\frac{k}{2}\right)^{-2}. \tag{11}$$

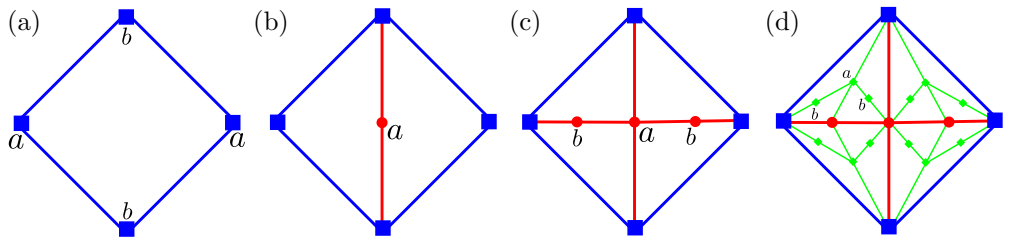

FIG. 2. (Color online) Hierarchical rule to construct the contact network for $m = n = 0$. (a) One starts with a loop of four nodes (two a and two b nodes) in a loop arrangement. (b) A new a node is added to the center of the loop and connected to the b nodes on the top and bottom of the loop, dividing it into two loops. (c) Two new b nodes are also added, one inside of each loop and connected to the two closest a nodes. The initial loop is now divided into four equal loops. (d) The new generation is constructed in the same way inside each loop.

The total degree distribution $P(k,g)$ is then

$$P(k,g) = \frac{\Delta N_a(g_{0a}(k)) + \Delta N_b(g_{0b}(k))}{N(g)} = \frac{3}{2}\frac{4^g}{4^g - 1}\left(\frac{k}{2}\right)^{-2}. \tag{12}$$

In the limit $g \to \infty$,

$$P_a(k) = 3\left(\frac{k}{2}\right)^{-2}, \tag{13}$$

$$P_b(k) = \frac{3}{4}\left(\frac{k}{2}\right)^{-2}, \tag{14}$$

$$P(k) = \frac{3}{2}\left(\frac{k}{2}\right)^{-2}. \tag{15}$$

Thus, the degree distribution scales as $P(k) \propto k^{-\gamma}$, with $\gamma = 2$, corresponding to a scale-free network. This exponent is larger than the one obtained for the Apollonian network, where $\gamma = \frac{\ln 3}{\ln 2} \approx 1.585$ [4]. Note that the a/b asymmetry disappears when one considers the two topological identical loops in the entire unit cell, because the a nodes in the top loop correspond to the b nodes in the bottom one.

C. Shortest paths and clustering coefficient

Spatial, self-similar networks are expected to exhibit some form of small-world behavior due to the confinement of connections [5], which is, for example, the case of the Apollonian network [15]. Numerically, this can be checked by analyzing the size dependence of the average shortest path l, defined as the average minimum number of links necessary to form a connecting path between pairs of nodes in the network. Figure 3 shows that $l = a \ln N + b$, where a and b are constants, corresponding to a logarithmic scaling, as expected for small-world networks [16].

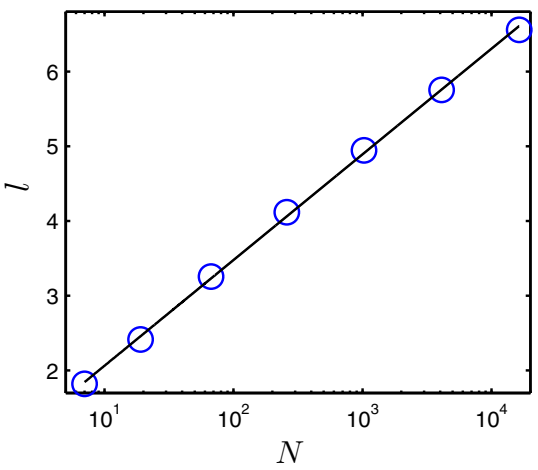

FIG. 3. (Color online) Size dependence of the average shortest path l, for the contact network of bearings of $m = n = 0$, where N is the number of nodes. As expected for small-world networks, the shortest path scales logarithmically with the number of nodes, over more than three orders of magnitude. By regression, we estimate $l = 0.61 \ln N + 0.65$.

Small-world networks are typically highly clustered [16]. To quantify the degree of clustering one measures the clustering coefficient C, defined for each node as the fraction of pairs of neighbors that are directly connected, forming a triangle. In the case of bearings, all loops have an even number of nodes, the contact network is bipartite, and two neighbors of a node are never directly connected. Lind *et al.* [17] proposed a new clustering coefficient for bipartite networks, C_4, defined as the fraction of pairs that are indirectly connected through one single node, forming a loop. Then, for a node of degree k,

$$C_4 = \frac{\text{No. of indirect connections between neighbors}}{k(k-1)/2}. \tag{16}$$

In the following we use this definition. First, we calculate $C_{4a/b}(t)$, the clustering coefficient of an a/b node that was added to the network t generations before. At each iteration, the degree of every node is doubled, by adding new neighbors. Each new neighbor is connected via a new node to other two neighbors (see Fig. 2). Thus, the number of indirectly connected pairs of neighbors increases at each generation by twice the node degree. Every new a node has degree 4 and from its six different pairs of neighbors, five are indirectly connected. Every new b node has degree 2 and its pair of neighbors is always indirectly connected. By summing over generations, one gets, for a nodes,

$$C_{4a}(t) = \frac{5 + \sum_{i=0}^{t-1} 2 \times k_a(i)}{k_a(t)(k_a(t)-1)/2} = \frac{3}{2}2^{-t} - \frac{2}{4 \times 2^t - 1}, \tag{17}$$

and for b nodes,

$$C_{4b}(t) = \frac{1 + \sum_{i=0}^{t-1} 2 \times k_b(i)}{k_b(t)(k_b(t)-1)/2} = 3 \times 2^{-t} - \frac{2}{2 \times 2^t - 1}, \tag{18}$$

where we employed Eqs. (6) and (7). Once again, note that the a/b asymmetry is only observed when we solely consider one loop. For the entire stripe, the top and bottom loops of the unit cell are equivalent, but the a nodes of the top loop are b nodes of the bottom one. Thus, when the entire unit cell is considered, the network is completely symmetric with respect to a and b. Both coefficients tend to zero as $C_4(t) \sim 2^{-t}$ for $t \to \infty$. The clustering of the entire network can be evaluated from the average over all nodes,

$$C_4(g) = \sum_{t=1}^{g} \frac{\Delta N_a(t) C_{4a}(g-t) + \Delta N_b(t) C_{4b}(g-t)}{N(g)}. \tag{19}$$

We evaluate this sum numerically as shown in Fig. 4, for different numbers of nodes in the network, and obtain that $C_4 \approx 0.8625$ in the thermodynamic limit.

D. Bond percolation

We now study bond percolation on a network corresponding to a unit cell of the stripe, consisting of two initial squares sharing one link (see Fig. 1). We focus on the existence of a spanning cluster between the two nodes representing the top and bottom surfaces, respectively. To compute the percolation threshold, we performed Monte Carlo simulations

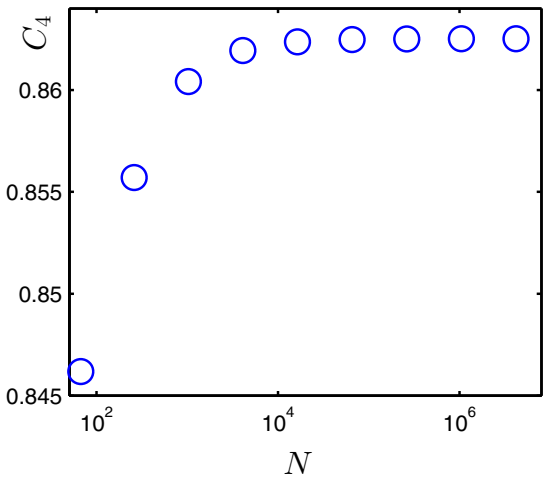

FIG. 4. (Color online) Clustering coefficient C_4 for the contact network of bearings of $m = n = 0$ as a function of the number of nodes, N. The values of C_4 were obtained by numerically evaluating the sum (19). The value of the clustering coefficient converges towards $\approx$0.8625 in the thermodynamic limit.

for different values of bond occupation probability p and network size N. We estimate the threshold p_c as the value of p at which the probability of spanning $P(p_c) = 1/2$, defined as the probability that the bottom and the top nodes of the network are connected through occupied bonds. We start with a given value of $p = p^*$ and calculate the spanning probability $P(p^*)$. We employ the bisection method iteratively until $|P(p^* - 1/2)| < 10^{-3}$. Figure 5 shows the size dependence of the estimated value of p_c, where one clearly sees that p_c vanishes in the thermodynamic limit. Asymptotically, the decay follows a power-law $p_c \sim N^{-\frac{1}{2\nu}}$, with $\nu \approx 7$. The same threshold is observed for the Apollonian network and other scale-free networks with $\gamma < 3$. However, the convergence to the thermodynamic value is much slower here than for the Apollonian network, where $\nu \approx 3$ [4].

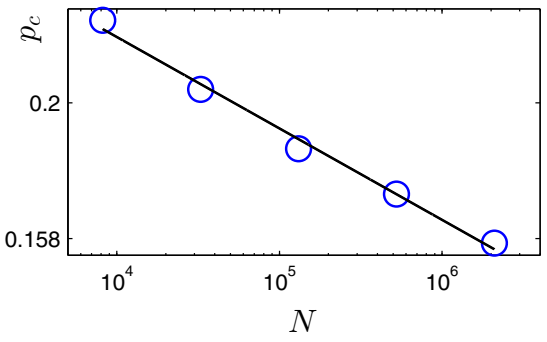

FIG. 5. (Color online) Dependence of the percolation threshold p_c on the network size N. We estimate the threshold p_c as the value of p at which the probability of spanning $P(p_c)$ is 1/2. We applied the bisection method and simulated different values of p^* until $|P(p^*) - 1/2| < 10^{-3}$. The black line corresponds to the least-squares fit to the data, $\log p_c \sim -\frac{1}{2\nu} \log N$, with exponent $\nu = 7 \pm 1$ and coefficient of determination 0.992.

III. GENERAL CASE

A. The network construction

We now consider the general case of the contact network for a bearing in the first family for loops of size 4 with any m and n. Figure 6 shows examples of bearings generated with different m and n, with the respective contact network on top. For all cases, the unit cell consists of loops of size 4 with the largest disks, including the top and bottom surfaces, respectively. However, the number of such loops varies with m and n and the rotation symmetry is broken for $m \neq n$. At each iteration the number of vertical and horizontal new loops constructed inside each loop also depends on m and n, respectively. As summarized in Fig. 7, we first discuss how to determine the initial number of loops in the unit cell (left-hand panel) and proceed to discussing how to hierarchically fill each loop (right-hand panel).

For all values of m and n, the unit cell of the bearing consists of a top and a bottom part. The number of initial loops on top and bottom equals $n + 1$ and $m + 1$, respectively (see loops of blue-square nodes in Fig. 6 and left-hand panel in Fig. 7). Note that the (m,n) configuration is equivalent to the (n,m) configuration after a rotation of π around the point where the common edge of the top and bottom loops crosses the middle of the stripe. To hierarchically construct the network one starts with the $n + 1$ top and $m + 1$ bottom loops. Hereafter, we solely consider one top and a bottom loop (sharing one edge), as the construction of the other loops is straightforward. To form the first generation we first add $m + 1$ a nodes to the top loop and connect them to the two existing (lateral) b nodes, dividing the initial loop into $m + 2$ loops. Then, in each new loop, we add $n + 1$ b nodes and connect them to the top and bottom a nodes. We are left with $(n + 2)(m + 2)$ loops inside the top loop. Second, we construct the interior of the bottom loop. There, we start by adding $n + 1$ b nodes and connect them to the two existing (lateral) a nodes. Then, in each one of the new $n + 2$ loops we add $m + 1$ a nodes and connect them to the top and bottom b nodes. In the bottom, we are also left with $(n + 2)(m + 2)$ loops. Proceeding iteratively in the same way, we hierarchically construct the entire contact network of the space-filling bearing, for any m and n.

B. Degree distribution

We now provide an analytic expression for the degree distribution $P_{m,n}(k)$ for any m and n, following the same strategy as for $m = n = 0$ in Sec. II B. For simplicity, we restrict the calculation to networks inside a single loop (one initial top loop), as the total degree distribution of the unit cell is straightforwardly obtained as a weighted average of $P_{m,n}(k)$ and $P_{n,m}(k)$, corresponding to the degree distribution in the top and bottom loops, where the statistical weights are given by the initial fraction of top $(n + 1)$ and bottom $(m + 1)$ loops, respectively.

At each generation, $(n + 2)(m + 2)$ loops are constructed for every loop in the previous generation. As before, we neglect the initial set of nodes. At generation $g - 1$ there are $(n + 2)^{g-1}(m + 2)^{g-1}$ loops. Thus, from generations $g - 1$ to

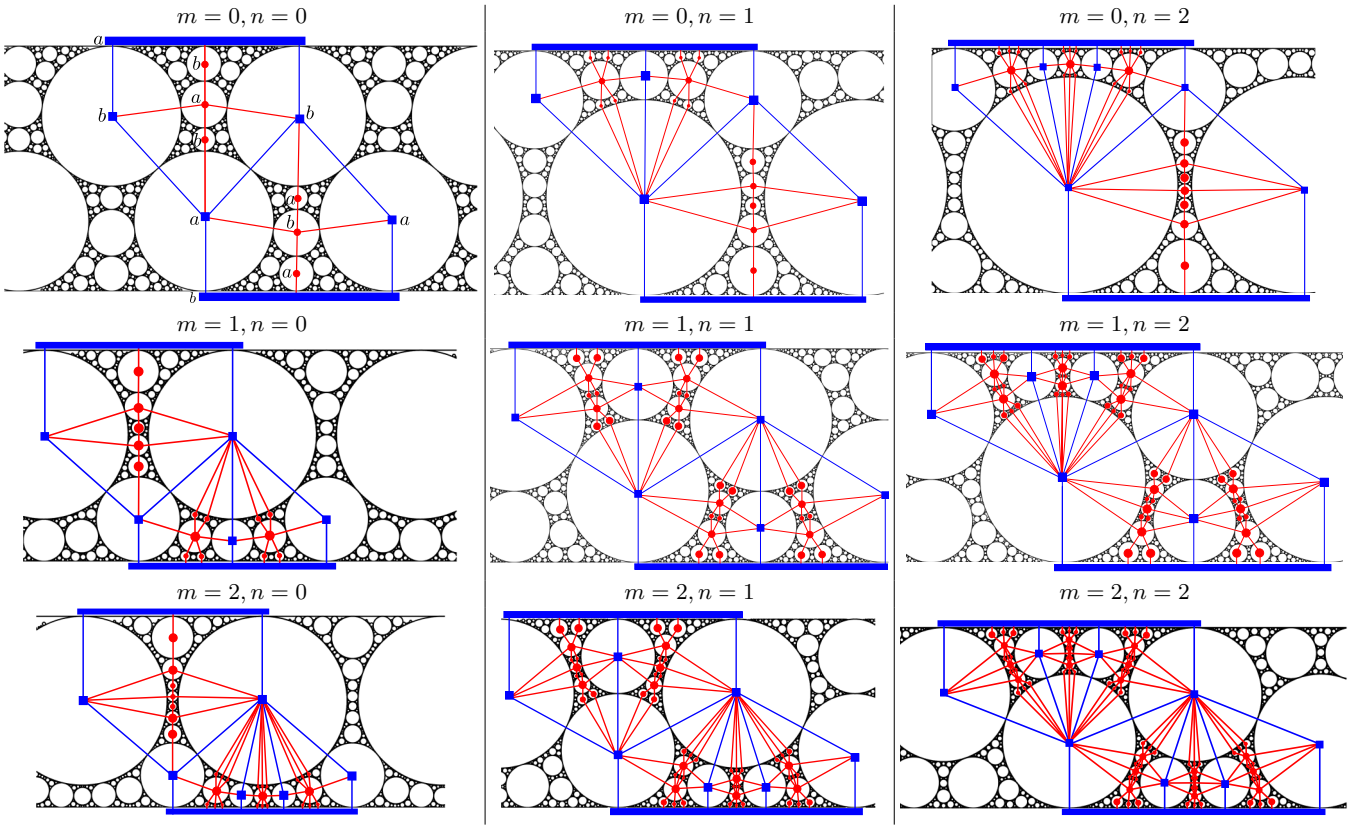

FIG. 6. (Color online) Examples of space-filling bearings of the first family, for different values of m and n.

g, the change in the number of a nodes is

$$\Delta N_a(g) = (m+1)[(n+2)(m+2)]^{g-1}, \tag{20}$$

and in the number of b nodes is

$$\Delta N_b(g) = (m+2)(n+1)[(n+2)(m+2)]^{g-1}, \tag{21}$$

corresponding to $(m+1)$ new a nodes and $(m+2)(n+1)$ new b nodes per loop. The number of nodes at generation g is then

$$\begin{aligned} N_a(g) &= (m+1)\sum_{t=1}^{g}[(n+2)(m+2)]^{t-1} \\ &= \frac{(m+1)([(n+2)(m+2)]^g - 1)}{(n+2)(m+2)-1} \end{aligned} \tag{22}$$

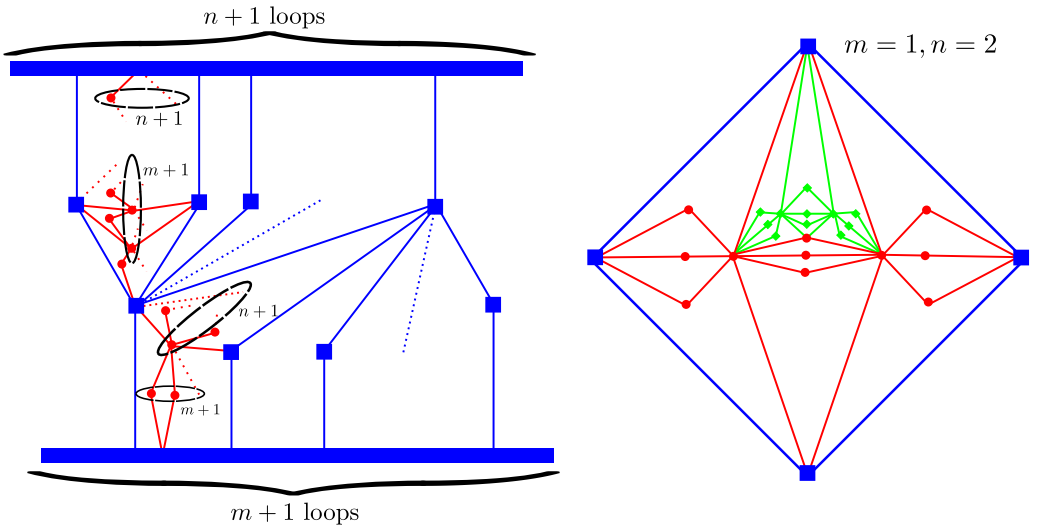

FIG. 7. (Color online) Left: A sketch of the initial network setup (blue, sites drawn as squares) and the first generation in the general case (red, sites as dots). Right: The first two generations and part of the second (green) for $m = 1$ and $n = 2$.

and

$$N_b(g) = (m+2)(n+1)\sum_{t=1}^{g}[(n+2)(m+2)]^{t-1} = \frac{(m+2)(n+1)([(n+2)(m+2)]^g - 1)}{(n+2)(m+2)-1}, \quad (23)$$

respectively. The total number of nodes, N, is

$$N(g) = N_a(g) + N_b(g) = [(n+2)(m+2)]^g - 1. \quad (24)$$

The degree k of a node increases monotonically with the generation. An a node has initially degree $2(n+2)$ and its degree increases by a factor of $n+2$ at each generation. Thus, at generation g, the degree of an a node added at generation g_0 is

$$k_a(g-g_0) = 2(n+2)^{g-g_0+1}. \quad (25)$$

A b node has initially degree 2 and its degree increases by a factor of $m+2$ at each generation. Thus, at generation g, the degree of a b node added at generation g_0 is

$$k_b(g-g_0) = 2(m+2)^{g-g_0}. \quad (26)$$

Consequently, the node of degree k at generation g that was added at generation g_0 is given by

$$g - g_{0a}(k) = \frac{\ln(k/2)}{\ln(n+2)} - 1 \quad (27)$$

for a nodes and

$$g - g_{0b}(k) = \frac{\ln(k/2)}{\ln(m+2)} \quad (28)$$

for b nodes. The degree distribution for the a nodes in the loop is then

$$P^a_{m,n}(k,g) = \frac{\Delta N_a(g_{0a}(k))}{N_a(g)} = [(n+2)(m+2)-1] f_{m,n}(g)\left(\frac{k}{2}\right)^{-[1+\frac{\ln(m+2)}{\ln(n+2)}]}, \quad (29)$$

where

$$f_{m,n}(g) = \frac{[(n+2)(m+2)]^g}{[(n+2)(m+2)]^g - 1}. \quad (30)$$

For the b nodes it is

$$P^b_{m,n}(k,g) = \frac{\Delta N_b(g_{0b}(k))}{N_b(g)} = \frac{(n+2)(m+2)-1}{(n+2)(m+2)} f_{m,n}(g)\left(\frac{k}{2}\right)^{-[1+\frac{\ln(n+2)}{\ln(m+2)}]}. \quad (31)$$

And the total degree distribution $P_{m,n}(k,g)$ is

$$P_{m,n}(k,g) = \frac{\Delta N_a(g_{0a}(k)) + \Delta N_b(g_{0b}(k))}{N(g)} = f_{m,n}(g)\left[(m+1)\left(\frac{k}{2}\right)^{-[1+\frac{\ln(m+2)}{\ln(n+2)}]} + \frac{n+1}{n+2}\left(\frac{k}{2}\right)^{-[1+\frac{\ln(n+2)}{\ln(m+2)}]}\right]. \quad (32)$$

In the limit $g \to \infty$,

$$P_{m,n}(k) = (m+1)\left(\frac{k}{2}\right)^{-[1+\frac{\ln(m+2)}{\ln(n+2)}]} + \frac{n+1}{n+2}\left(\frac{k}{2}\right)^{-[1+\frac{\ln(n+2)}{\ln(m+2)}]}. \quad (33)$$

When $m = n$, $\gamma = 2$ is recovered [5]. For $m \neq n$, the degree distribution is a sum of two power laws. Asymptotically, for $k \to \infty$, $P_{m,n}(k)$ is dominated by the term with the smallest exponent and thus

$$\gamma = \min\left\{1 + \frac{\ln(m+2)}{\ln(n+2)}, 1 + \frac{\ln(n+2)}{\ln(m+2)}\right\}. \quad (34)$$

The contact network of a bearing is always a scale-free network of $1 < \gamma \leqslant 2$, as shown in Fig. 8.

Note that the degree exponent is symmetric to permutations of m and n. The degree distribution of the entire unit cell is

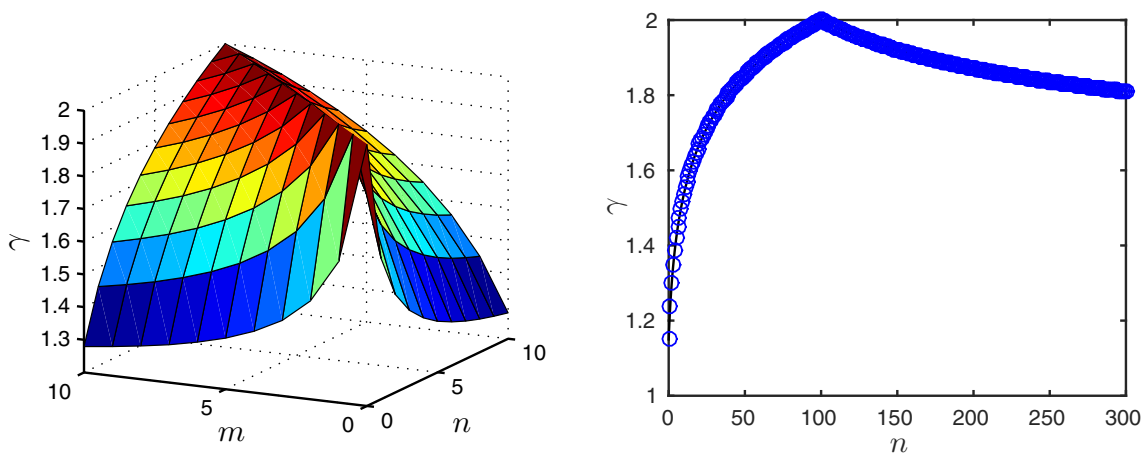

FIG. 8. (Color online) Left: Degree exponent γ as a function of m and n. Note that $1 < \gamma \leqslant 2$ and $\gamma = 2$ for $m = n$. Right: Degree exponent γ as a function of n for $m = 100$.

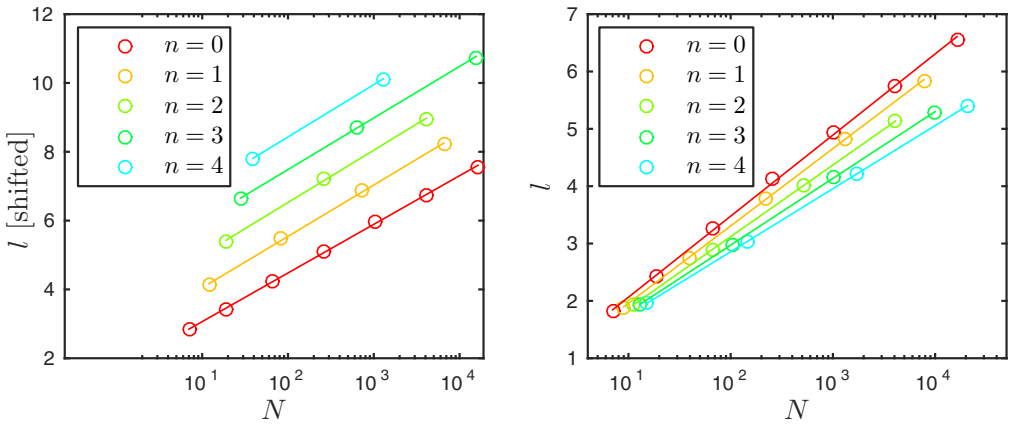

FIG. 9. (Color online) Left: Average shortest path l as a function of the number of nodes, N, for $n = m$. Lines were shifted vertically by adding n for better visualization. Right: Average shortest path l as a function of the number of sites, N, for $m = 0$. Lines were also shifted vertically. The lines are just guides to the eye.

symmetric at every generation as it is given by

$$P(k) = \frac{(n+1)P_{m,n}(k) + (m+1)P_{n,m}(k)}{m+n+2} = \frac{\left[(n+1)(m+1) + \frac{(m+1)^2}{m+2}\right]\left(\frac{k}{2}\right)^{-\left[1+\frac{\ln(m+2)}{\ln(n+2)}\right]}}{m+n+2} + \frac{\left[\frac{(n+1)^2}{n+2} + (n+1)(m+1)\right]\left(\frac{k}{2}\right)^{-\left[1+\frac{\ln(n+2)}{\ln(m+2)}\right]}}{m+n+2}. \quad (35)$$

C. Shortest path and clustering coefficient

We numerically analyze the size dependence of the average shortest path l for all combinations of $n,m = 0,1,2,3,4$. For all cases, we find a logarithmic scaling of l with the number of nodes, consistent with small-world networks. For $m = n$ we find that the prefactor of the logarithmic scaling is independent of the value of the indices, as also observed for γ. If $m \neq n$, then the prefactor changes with m and n as shown in Fig. 9; for example, for fixed $m = 0$, the prefactor decreases with n.

Next, we calculate C_4. A new a node has $(n+3)(n+2)-1$ pairs of neighboring b nodes connected indirectly through one a node. At each generation, when new neighbors are added to each loop adjacent to this a node, the number of connected pairs increases by $(n+3)(n+2)/2 - 1$. Hence, an a node that was added to the network at generation g_0, and is part of the network for $t = g - g_0$ generations, has a clustering coefficient

$$C_{4a}(t) = \frac{(n+3)(n+2) - 1 + \left[\frac{(n+3)(n+2)-1}{2} - 1\right]\sum_{i=0}^{t-1} k_a(i)}{k_a(t)(k_a(t)-1)/2} = \frac{(n+3)(n+2)-1}{(n+2)^{t+1}[2(n+2)^{t+1}-1]} + \frac{2(n+2)\left[\frac{(n+3)(n+2)-1}{2} - 1\right]\frac{(n+2)^t-1}{n+1}}{(n+2)^{t+1}[2(n+2)^{t+1}-1]} \sim (n+2)^{-t} \text{ as } t \to \infty.$$

Initially, for b nodes there is only one pair of neighbors indirectly connected and $\frac{(m+3)(m+2)}{2} - 1$ connections are added per adjacent loop at each iteration. Thus,

$$C_{4b}(t) = \frac{1 + \left[\frac{(m+3)(m+2)-1}{2} - 1\right]\sum_{i=0}^{t-1} k_b(i)}{k_b(t)(k_b(t)-1)/2} = \frac{1 + 2\left[\frac{(m+3)(m+2)-1}{2} - 1\right]\frac{(m+2)^t-1}{m+1}}{(m+2)^t(2(m+2)^t-1)} \sim (m+2)^{-t} \text{ as } t \to \infty.$$

The argument of the power law is different for a and b nodes as it depends on n and m, respectively. Both C_{4a} and C_{4b} asymptotically vanish. The faster the degree of a node type grows the faster its C_4 falls off.

D. Bond percolation

We performed simulations of the bond percolation model on a unit cell for different pairs of indices m,n. As in Sec. II D, we define the spanning cluster as a set of connected nodes that includes the top and bottom surfaces. Note that the top and bottom surfaces correspond to different types of nodes, a and b, respectively (see Fig. 6).

For all considered values of m and n we find that the percolation threshold p_c vanishes in the thermodynamic limit (infinite system size) and the estimator for the threshold scales as $p_c(N) \sim N^{-\frac{1}{2\nu}}$. Our results for $m = n$ suggest that ν does not change with the bearing indices (m and n), like we also found for the degree exponent γ in Sec. III B. Since the growth constant of the number of nodes with the generation increases with m and n, we refrain from performing a detailed size-dependence analysis to obtain ν with high precision.

IV. FINAL REMARKS

We studied the contact network of space-filling bearings of loops of size 4 in the first family. We proposed a hierarchical rule to construct the network and provided analytic expressions for the degree distribution and clustering coefficient. We also studied numerically the shortest path and percolation properties. We showed that the exponent γ changes in the range $(1,2]$ and that is always 2 when $m = n$. Numerical

simulations also suggest that the correlation exponent ν for the percolation transition does not change with the bearing indices. Our networks are bipartite and we find that if $m \neq n$ the degree distribution of the two species scale with different exponents inside each loop. This is an example of an artificial hierarchical network exhibiting this property which has already been observed empirically for sexual networks [18].

We are proposing a method to generate deterministic hierarchical scale-free networks of different γ exponents, which are amenable to analytic treatment. As it was accomplished for the Apollonian network, possible extensions of our work include the study of their magnetic, spectral, and dynamical properties [19–21]. Other possibilities include the study of the networks of random space-filling or three-dimensional bearings, larger loops, and a second family of bearings.

Recently, there has been a sustained interest in packings of spheres and disks with a power-law distribution of radii, as it was shown experimentally that the transmission probability for such arrangements scales superdiffusively [22]. Studies of transmission probability require information about the spatial distribution of particles [23,24]. The hierarchical construction that we discuss here might provide a theoretical framework to study such optical systems.

ACKNOWLEDGMENTS

We acknowledge financial support from the ETH Risk Center, the Brazilian agencies CNPq, CAPES, FUNCAP, the Brazilian Institute INCT-SC, ERC Advanced Grant No. FP7-319968 of the European Research Council, and the Portuguese Foundation for Science and Technology (FCT) under the Contracts No. IF/00255/2013 and No. UID/FIS/00618/2013. J.J.K. thanks "Studienstiftung des Deutschen Volkes" for support through a scholarship.

[1] H. J. Herrmann, G. Mantica, and D. Bessis, Phys. Rev. Lett. **65**, 3223 (1990).
[2] C. Lomnitz, Bull. Seismol. Soc. Am. **72**, 1441 (1982).
[3] R. M. Baram, P. G. Lind, J. S. Andrade, Jr., and H. J. Herrmann, Europhys. Lett. **91**, 28006 (2010).
[4] J. S. Andrade, Jr., H. J. Herrmann, R. F. S. Andrade, and L. R. da Silva, Phys. Rev. Lett. **94**, 018702 (2005).
[5] J. P. K. Doye and C. P. Massen, Phys. Rev. E **71**, 016128 (2005).
[6] R. F. S. Andrade and H. J. Herrmann, Phys. Rev. E **71**, 056131 (2005).
[7] R. F. S. Andrade, J. S. Andrade, Jr., and H. J. Herrmann, Phys. Rev. E **79**, 036105 (2009).
[8] N. A. M. Araújo, R. F. S. Andrade, and H. J. Herrmann, Phys. Rev. E **82**, 046109 (2010).
[9] R. F. S. Andrade and J. G. V. Miranda, Phys. A (Amsterdam, Neth.) **356**, 1 (2005).
[10] G. L. Pellegrini, L. de Arcangelis, H. J. Herrmann, and C. Perrone-Capano, Phys. Rev. E **76**, 016107 (2007).
[11] Z. Zhang, J. Guan, W. Xie, and S. Zhou, Europhys. Lett. **86**, 10006 (2009).
[12] Z. Zhang and S. Zhou, Phys. A (Amsterdam, Neth.) **380**, 621 (2007).
[13] R. C. Hidalgo, C. U. Grosse, F. Kun, H. W. Reinhardt, and H. J. Herrmann, Phys. Rev. Lett. **89**, 205501 (2002).
[14] N. A. M. Araújo, H. Seybold, R. M. Baram, H. J. Herrmann, and J. S. Andrade, Jr., Phys. Rev. Lett. **110**, 064106 (2013).
[15] Z. Zhang, L. Chen, S. Zhou, L. Fang, J. Guan, and T. Zou, Phys. Rev. E **77**, 017102 (2008).
[16] D. J. Watts and S. H. Strogatz, Nature (London) **393**, 440 (1998).
[17] P. G. Lind, M. C. Gonzalez, and H. J. Herrmann, Phys. Rev. E **72**, 056127 (2005).
[18] B. F. Blasio, A. Svensson, and F. Liljeros, Proc. Natl. Acad. Sci. U. S. A. **104**, 10762 (2007).
[19] A. A. Moreira, D. R. Paula, R. N. Costa Filho, and J. S. Andrade, Jr., Phys. Rev. E **73**, 065101(R) (2006).
[20] I. N. de Oliveira, F. A. B. F. de Moura, M. L. Lyra, J. S. Andrade, Jr., and E. L. Albuquerque, Phys. Rev. E **79**, 016104 (2009).
[21] I. N. de Oliveira, F. A. B. F. de Moura, M. L. Lyra, J. S. Andrade, Jr., and E. L. Albuquerque, Phys. Rev. E **81**, 030104(R) (2010).
[22] P. Barthelemy, J. Bertolotti, and D. S. Wiersma, Nature (London) **453**, 495 (2008).
[23] C. W. Groth, A. R. Akhmerov, and C. W. J. Beenakker, Phys. Rev. E **85**, 021138 (2012).
[24] R. Burioni, E. Ubaldi, and A. Vezzani, Phys. Rev. E **89**, 022135 (2014).